Bringing the Nanolaboratory Inside Electron Microscopes

1932-4510/08/$25.00©2008IEEE

A NANOLABORATORY IS ONE OF THE SYSTEMS TO REALIZE VARIOUS nanoscale fabrications and assemblies to develop novel nanodevices to integrate borderless technologies based on a nanorobotic manipulation system. We have presented the nanolaboratory inside electron microscopes including a transmission electron microscope (TEM), scanning electron microscope (SEM), and environmental-SEM (E-SEM) for three-dimensional (3-D) and real-time nanomanipulation, nanoinstrumentation, and nanoassembly.

The following is a presentation of our current work of nanomanipulation and nanoassembly based on the hybrid nanorobotic manipulation inside a TEM and an SEM toward carbon nanotube (CNT) applications. Single cell stiffness measurement has been also presented based on the nanorobotic manipulation system inside an E-SEM.

TOP DOWN, BOTTOM UP

Nanotechnology has an important role in the combinations of the top-down and bottom-up approaches. The possibility to control the structure of matter, atom by atom, was first seriously discussed by Richard Feynman in 1959, in his lecture, "There's Plenty of Room at the Bottom," which is now labeled "Nanotechnology" [1]. The wide scale controlled devices from atomic scale to meter scale are expected to be realized in the near future (Figure 1).

Molecular nanoassembly is one of the most impressive nanotechnologies. E. Drexler proposes the machine-phase nanosystems based on self-replicative molecular assembler via mechanosynthesis (Figure 2) [2], [3]. The molecular machines might be realized as effective mechanical systems in near future. Assemblers, which are one of the molecular machines, might be created as a general purpose manufacturing device that is able to build a wide range of useful products as well as copies of itself (self-replication).

To fill the gap between top-down and bottom-up approaches, nanomanipulations, which realize controlling the position at the nanometer scale, are considered to be promising (Figure 3). It might be a key technology to lead the appearance of replication-based assemblers. The top-down fabrication process, or micromachining, provides numbers of nanometer structures at once. The bottom-up fabrication process, or chemical synthesis, such as self-assembly or super-molecule techniques, also provides numerous nanometer structures. Both approaches reach nanometer scale with the limitations of physical/chemical aspects at present. Hence, the technology to fill its gap is considered to be one of the important at this moment.

NANOLABORATORY BASED ON NANOROBOTIC MANIPULATION

Since the year 2000, we have been proposing a nanolaboratory based on a nanorobotic manipulation system. [4]. It is one of the systems to realize various nanoscale fabrications and assemblies to develop novel nanodevices to integrate borderless technologies

TEMs and SEMs focus on hybrid nanorobotic manipulation for carbon nanotube applications.

TOSHIO FUKUDA, MASAHIRO NAKAJIMA, POU LIU, AND MOHD RIDZUAN AHMAD

Digital Object Identifier 10.1109/MNANO.2008.925517

based on a nanorobotic manipulation system. It is readily applied to the scientific exploration of mesoscopic phenomena and the construction of prototype nanodevices. It would be one of the most significant enabling technologies to realize the manipulation and fabrication technology with individual atoms and molecules for the assembly of devices.

Recently, the investigation of nanoelectromechanical systems (NEMS) has attracted much attention [5]–[8]. It is expected to realize high-integrated, miniaturized, and multifunctional devices for various applications. One effective way is the direct usage of the bottom-up fabricated nanostructures. The nanolaboratory is rapidly prototyping ways to construct such high-precision systems under controlled environments. Figure 3 shows the strategies of a nanolaboratory based on a nanorobotic manipulation system. The applications under dry or semi-wet conditions can be done through a TEM/SEM or E-SEM nanorobotic manipulation system.

The nanolaboratory is a fundamental technology for property characterization of nano materials, structures, and mechanisms; for the fabrication of nano building blocks; and for the assembly of nano devices.

The nanolaboratory can be applied for nanoassembly and nanoinstrumentation, such as nanohandling, nanomodification, and nanowiring using various nanomaterials under microscopes through nanofabrication techniques based on a nanorobotic manipulation system (Figure 4).

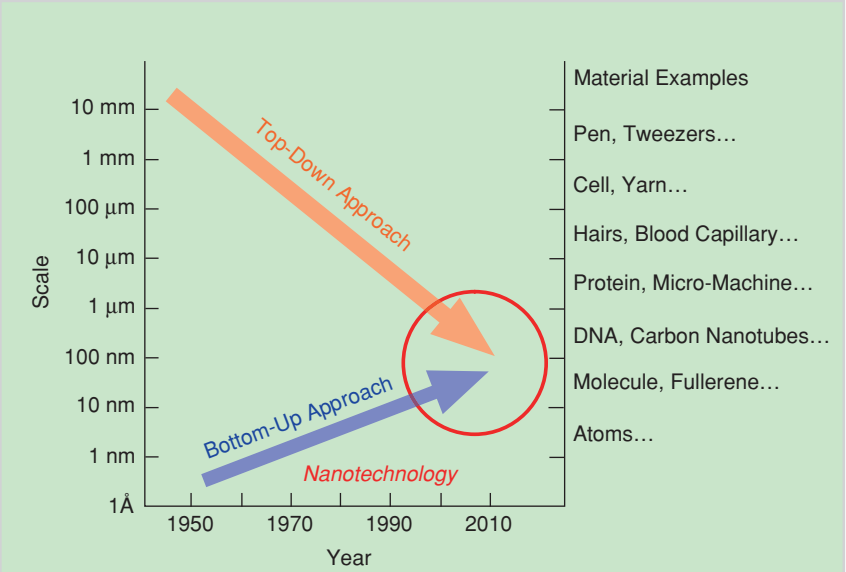

FIGURE 1 Schematic diagram of nanotechnology (top down and bottom up).

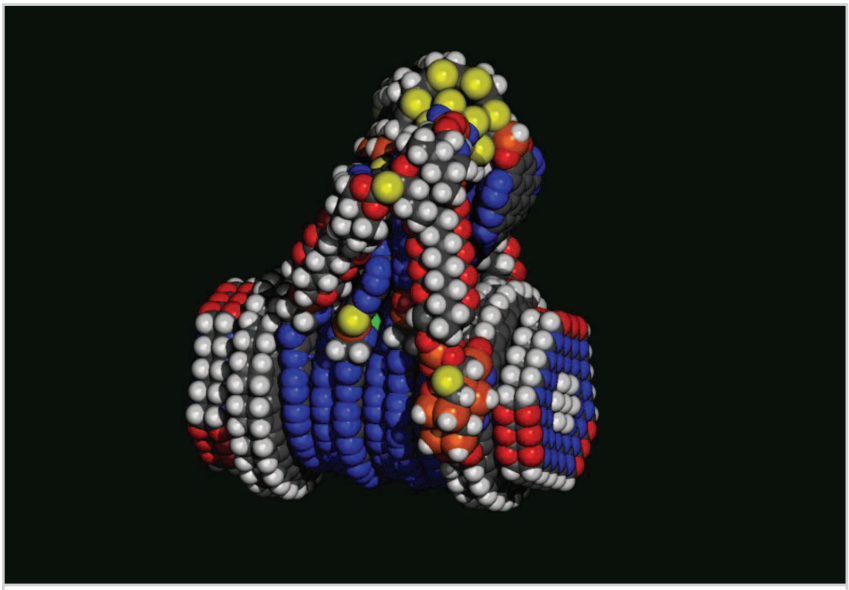

FIGURE 2 A fine-motion controller for molecular assembly—a 100 nm-scale manipualtor arm [3]. © Institute for Molecular Manufacturing (www.imm.org). Image used with permission.

NANOROBOTIC MANIPULATIONS

Nanorobotic manipulation—nanomanipulation—has received much more attention since it is an effective strategy for the property characterizations of individual nanoscale materials and the construction of nanoscale devices (Figure 5) [9]. To manipulate nano-scale objects, one must observe them with a resolution higher than nanoscale. Hence, the manipulators and observation systems, microscopes in general, are necessary for nanomanipulations.

Figure 6 shows the strategies of nanomanipulations with various kinds of microscopes. As shown in Table 1, the nanomanipulation under various microscopes for 2-D/3-D nanomanipulations. The optical microscope (OM) is one of the most historical and basic microscopes. However, its resolution is limited to ~100 nm due to the diffraction limit of optical wavelength (~400– ~800 nm) explained by Abbe's law. The special techniques (e.g., using evanescent light or fluorescent light) are needed for the observation under nanometer scale objects [10]. To observe the nanoscale objects, a resolution higher than nanoscale is required. Until now, the scanning probe microscopes (SPMs) and electron microscopes are readily used for the nanomanipulation techniques. They may be the core-most part of nanotechnology. One of the attractive future applications of nanomanipulation is to realize the ultimate goal of nanotechnology.

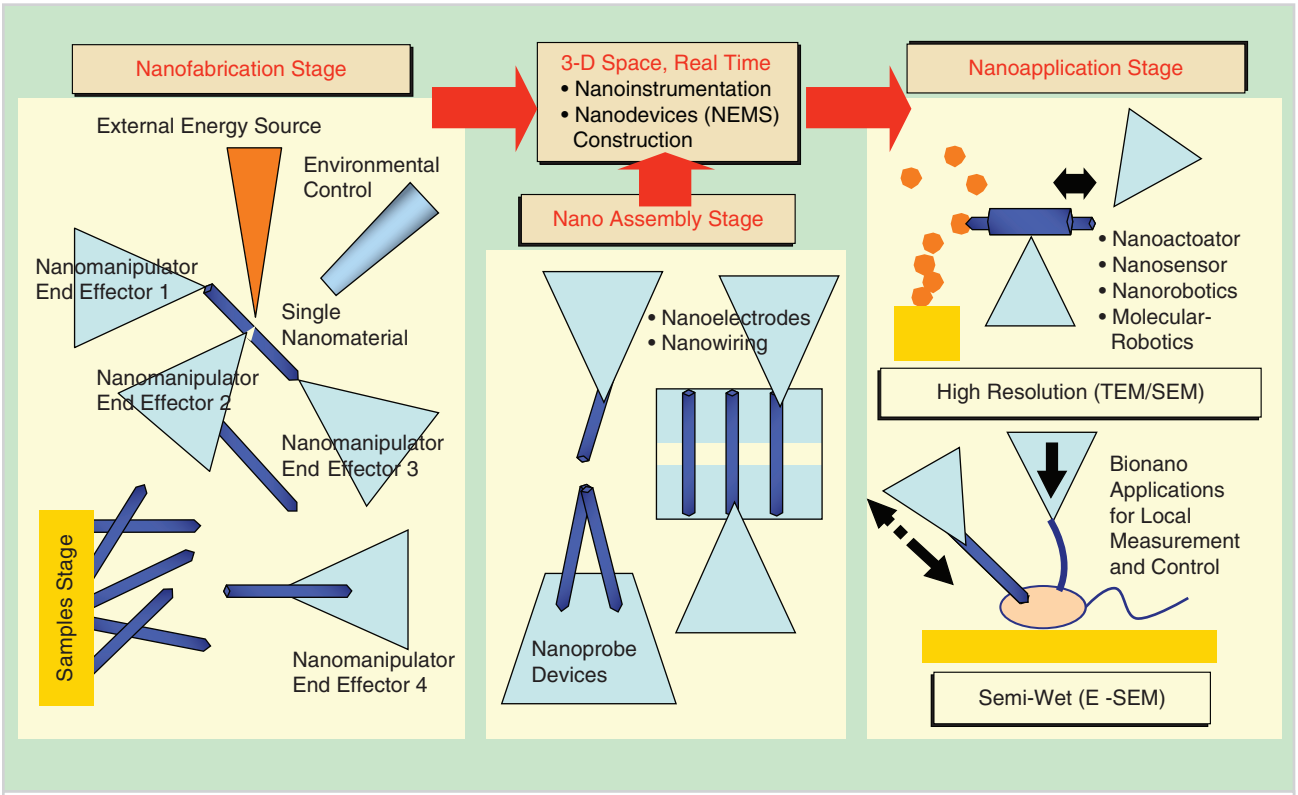

FIGURE 3 Strategies of nanolaboratory based on a multiple nanorobotic manipulation system under 3-D space and realtime observation.

NANOROBOTIC MANIPULATION SYSTEMS BASED ON SCANNING PROBE MICROSCOPES

The SPMs, like scanning tunnelling microscopes (STMs) or atomic force microscopes (AFMs), have functions of both observation and manipulation. Their high resolution makes them capable of atomic manipulation. In 1990, Eigler and Schweize demonstrated the first atom practice nanomanipulation with scanning tunnelling microscope (STM) [11]. They applied an STM at low temperature (4K) to position individual xenon atoms on a single-crystal, nickel surface with atomic precision. The manipulation enabled them to fabricate rudimentary structures of their own design, atom by atom. The result image atoms were moved to form the three letters "IBM." This work shows the impact feasibility of the control of the atoms through nanomanipulation.

Hosoki et. al. also demonstrated the atomic letter by STM [12]. The MoS_2 atoms were evaporated by electric field at room temperature. Avouris et al. applied an AFM to bend and translate CNTs on a substrate [13]. The objects are pushed and

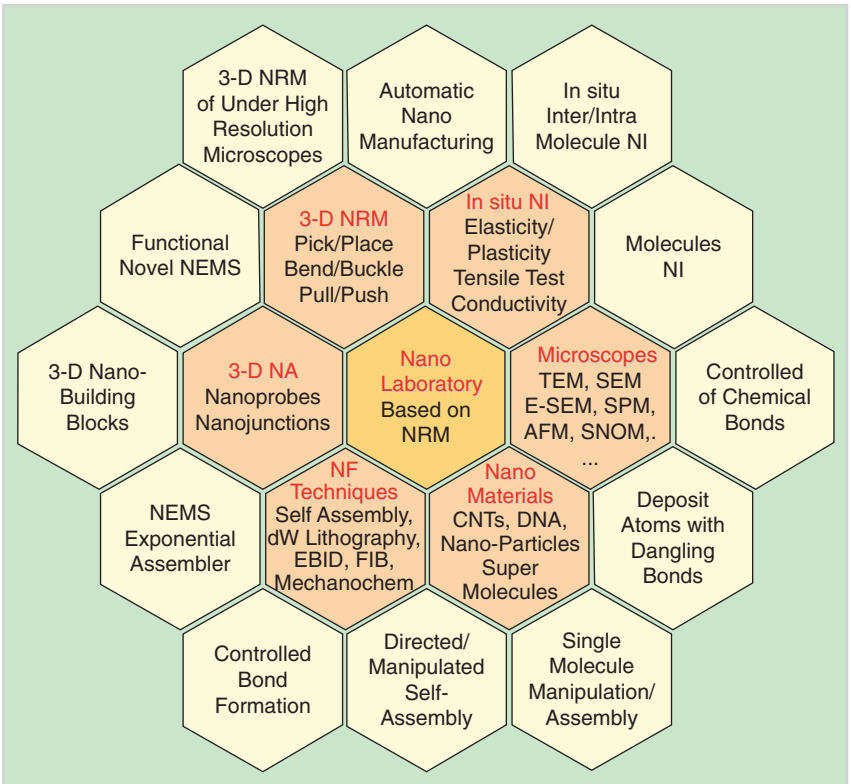

FIGURE 4 Various applications of nanolabratory based on a nanorobotic manipulation system. (NI: nano instrumentation, NA: nano assembly, NF: nano fabrication, NRM: nanorobotic manipulation, and NEMS: nanoelectromechanical system).

deformed by the tip of an AFM. They combined the techniques with an inverse process, namely straightening, by pushing along a bent tube, and realized the translation of a tube to another place. They also showed the assembly of two bent tubes and a straight one to form a "θ" letter. Ning Xi et al., at Michigan State University, developed an AFM-based nanomanipulation system with an interactive operation system [14], [15]. The system realized a real-time visual feedback during AFM-based nanomanipulation. They also proposed some physical models of the interaction among the AFM tip, substrate, and objects to feel the real-time interactive forces through a haptic system for the operator. It showed the "msu" character patterns by pushed nanoparticles on a glass surface. Metin Sitti et. al. also proposed the telenanorobotic system based on an AFM probe [16]. It consists of a piezoresistive AFM probe as a mechanical manipulation probe and topology sensor. A haptic device and virtual reality display are embedded for a force-feedback and a visual feedback system.

Normally, SPM systems have limits for the observation in a 2-D plane with a quite smooth surface. The observation area is limited and a long time is needed to get one image (more than mins). This limitation rises up as a 3-D nanomanipulation of nanostructures. Recently, T. Ando proposed a real-time AFM system for mainly biological molecules imaging in solution at nanometer scale resolutions [17], [18]. However, the observation area remains in several hundred nm range on the 2-D plane. In the future, this type of novel SPM system may work up an effective real-time nanomanipulation system.

NANOROBOTIC MANIPULATION SYSTEMS BASED ON ELECTRON MICROSCOPES

The observation space of SPMs is strictly limited and constrained in a plane, so the 3-D nanomanipulation is relatively difficult though these microscopes in a wide range. On the other hand, the electron microscopes provide atomic scale resolution with the electron beam whose wave length is less than ~0.1 Å. EMs are divided mainly into two types—SEMs and TEMs.

For nanomanipulation inside SEMs, Tsuchiya et. al., proposed nanomanufacturing world (NMW) [19]. NMW is a tabletop type micro-nano manipulation with assembly and fabrication simultaneously. The system has two chambers—assembly and marching chambers. In the machining chamber, a fast-atom-beam (FAB) source is effectively used for the micro-machining. In the assembly chamber, two SEMs are embedded for enough 3-D observation area. The two-unit remote manipulators are also embedded for the micro assembly with two probes. A micro house is constructed with two tungsten needle probes for demonstrations of the system.

S. Saito et. al. proposed an SEM manipulation system for an autonomous manipulation system [20], [21]. The system has the following features: 1) an optical microscope is equipped orthogonal to the SEM to obtain full 3-D information, 2) five degrees of freedom including rotation, and 3) a configuration where the probe tip is always located in the center of the field of view to guarantee the consistent acquisition of well-focused images.

M.F. Yu et al. presented the tensile strength of individual CNTs inside an SEM [22]. They presented the analysis of the stress-strain curves for individual CNTs to calculate the Young's modulus of them.

However the resolution of SEM, generally ~1 nm resolution, is approximately one order in magnitude lower than that of a TEM. High resolution and transmission images of TEMs are useful for measurement and evaluation of nanoscale objects. However, the specimen chamber and observation area of TEMs are too narrow to contain manipulators with complex functions, so special sample preparation techniques are needed. Before an ideal microscope was invented, it was a practical strategy to combine different microscopes so as to take advantage of both resolution and complexities.

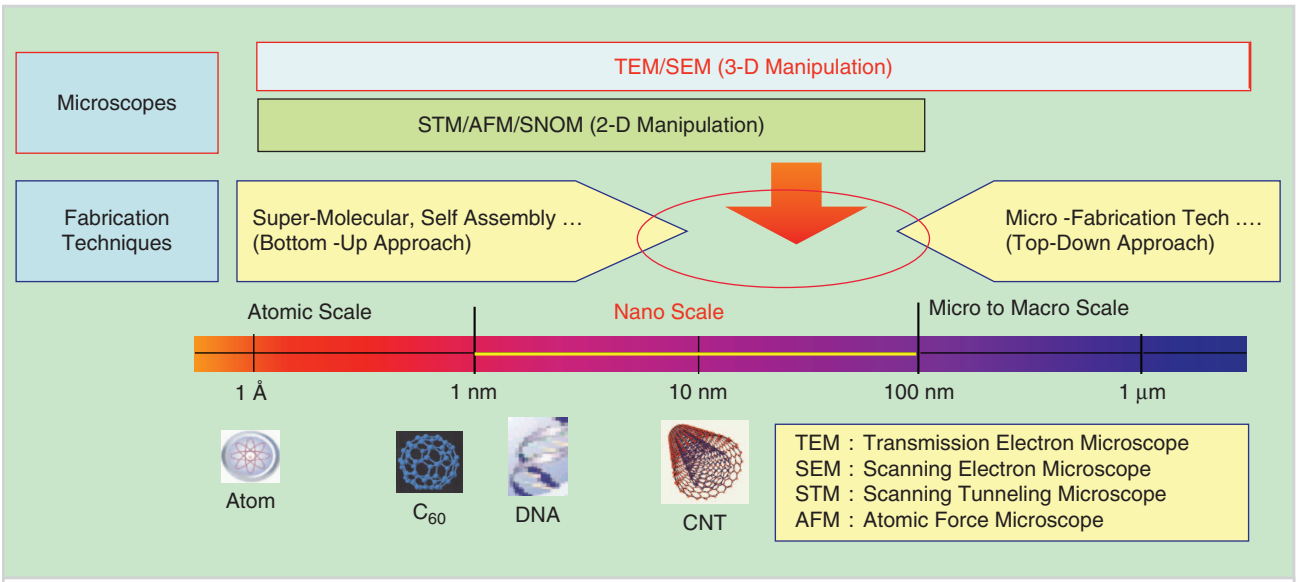

FIGURE 5 Nanorobotic manipulation system for nanodevices constructions.

Kizuka et.al. proposed the manipulation holder inside a high-resolution transmission electron microscope (HR-TEM). The manipulator was specially designed with atomic level positioning resolution [23]. For rough positioning, the motor and micro-gear mechanisms used the actuation. For precise positioning, a piezo-tube is used for three degrees of freedom (x-y-z) actuations. The maximum working area of rough positioning is ±1 mm. One of precise positioning is 1.2 μm in x direction, 11.4 μm in y direction, and ~11 μm in z direction. In situ fabrication of 2.6 nm single Au atomic nanowire is fabricated at the contact point of Au layers inside an HR-TEM [24]. Z.L. Wang demonstrated the quantitative measurement of the mechanical and electrical properties of nanobelts and nanotube in situ TEM [25].

HYBRID NANOROBOTIC MANIPULATION SYSTEM INSIDE SEMS AND TEMS

A hybrid nanorobotic manipulation system is integrated with a TEM nanorobotic manipulator (TEM manipulator) and a SEM nanorobotic manipulator (SEM manipulator) as a core system for the nanolaboratory. The nanomanipulations under EMs show their uniqueness to contain an independent nanomanipulator with real-time observation capability. The resolutions of TEMs can be readily used for the precise nanomanipulation and instrumentations. The issue with the TEM nanomanipulator is that its specimen chamber and observation area are too narrow to contain manipulators with complex functions.

We have proposed an exchangeable robotic manipulator between a field-emission SEM (FE-SEM) and a TEM [26], [27]. The strategy is named as hybrid nanomanipulation so as to differentiate it from those with only an exchangeable specimen holder. The most important feature of the manipulator is that it contains several passive DOFs, which makes it possible to perform relatively complex manipulations to keep compact the volume to be installed inside the narrow vacuum chamber of a TEM. A TEM nanomanipulator can be used inside a SEM and a TEM, and can be driven with SEM nanomanipulators for the setting of TEM samples. This system realizes an effective sample preparation inside a SEM with a wide enough working area, DOFs of manipulation [28], [29], and a high resolution measurement and evaluation of samples inside a TEM.

Figure 7 shows a schematic of the hybrid nanorobotic manipulation system. Figure 8 shows the overview of the constructed hybrid nanorobotic manipulation system.

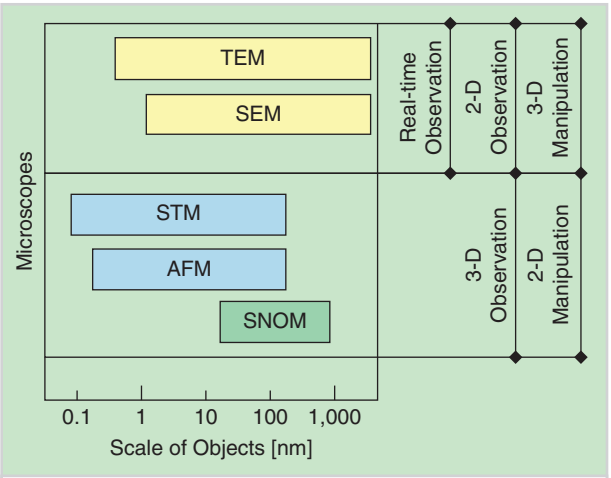

FIGURE 6 Strategies of Nanomanipulations under various microscopes.

IN SITU NANOFABRICATION AND NANOACTUATION OF TELESCOPING NANOTUBES

CNTs have been regarded as promising materials for nanostructures and nanodevices since their identification [30]. They have shown extraordinary mechanical properties and electronic properties [31], [32]. The elasticity of CNTs is considered to be ~1 TPa from theoretical analysis [33] and experimental results [34].

For the high-integrated, miniaturized, and functional NEMS, one of the effective ways is to use the bottom-up fabricated nanostructures directly. Basically, the CNTs have single or multirolled up cylindrical graphite sheets (like a Russian doll-like structure) with the interlayer space as ~0.34 nm [30], [35], [36], so there is the possibility to use their fine structures directly. For example, "telescoping carbon nanotube," which is fabricated by peeling off the outer layers of multi-walled-carbon-nanotubes (MWNTs), is one of the most interest nanostructures. J. Cummings et al. demonstrated that the pulling out of the inner core could be done so mechanically inside a transmission electron microscope (TEM) [37]. The inner core is automatically retracted inside the outer layers when the connection is freed by van der Waals force interactions.

A. M. Fennimore et al. demonstrated that MWNTs were used as the rotation axis of a silicon chip as rotational actuators [38]. Q. Zheng et al. proposed that telescoping MWNT has the possibility of gigahertz oscillator applications from the computational approaches by van der Waals interaction between inner core and outer layers effectively [39]. A.

TABLE 1 Nanomanipualtions under various microscopes for 2D/3D nanomanipulations.

MICROSCOPES	OBJECTS	METHODOLOGY OF NANOMANIPULATION	DIMENSIONS	REFS
SPM (STM)	Xenon atoms	van der Walls forces	2-D	[8]
SPM (STM)	MoS_2 atoms	Electric-field-evaporation	2-D	[9]
SPM (AFM)	CNTs	Contact pushing	2-D	[10]
SPM (AFM)	Nanoparticles, DNA	Contact pushing	2-D	[11], [12]
SPM (AFM)	DNA	Contact pushing	2-D	[13]
SEM	FAB materials	Contact pushing	3-D	[16]
SEM	CNTs, Nanowires	Contacts	2-D/3-D	[17]
SEM	Nanoparticles	Contacts	2-D/3-D	[18]
SEM	CNTs	Contacts	3-D	[19]
TEM	Au wires	Contacts	2-D	[20] [21]
TEM	Nanotubes, Nanobelts	Contacts	2-D/3-D	[22]

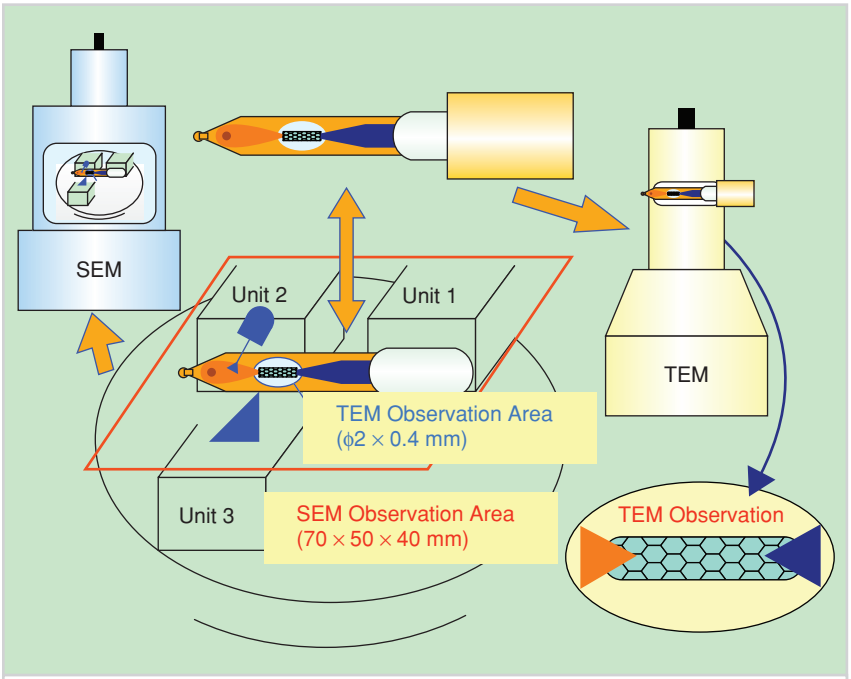

FIGURE 7 A schematic of a hybrid nanorobotic manipualtion system.

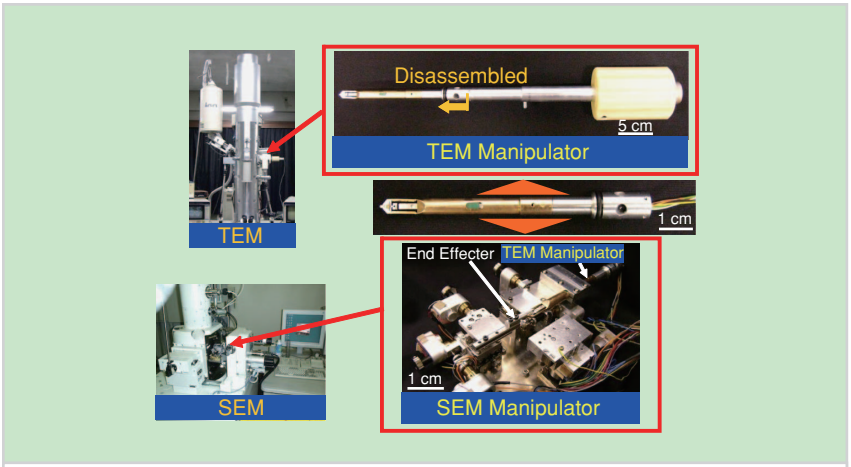

FIGURE 8 Overview of a constructed hybrid nanorobotic manipulation system.

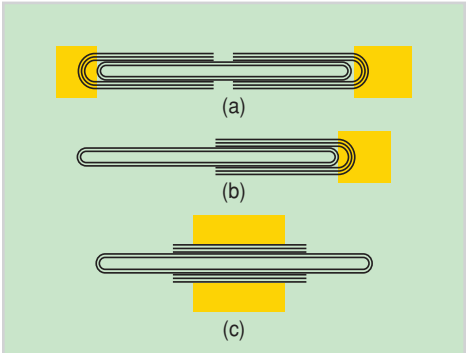

FIGURE 9 Schematic diagram of telescoping nanotubes. (a) Both sides fixed type, (b) one end opened type, and (c) both ends opened type.

Hansson et al. showed that the inner core of a telescoping carbon nanotube has a distributed intershell conductance for the sensing of the intershell distance [40].

In our work, we report on the direct observation of electrostatic actuation of a telescoping MWNT inside a TEM [41]. In previous works, Dong et al. proposed that the field emission current from a one-end opened telescoping MWNT can be used for position feedback control, and they carried out the experiment inside a SEM [42]. However, no direct confirmation of its actuation was observed because the charge up effects prevented the direct observation of the sample while applying the electric field. Here, we'll show the direct observation of its actuation under applied electrostatic field inside a TEM.

TELESCOPING NANOTUBES

The telescoping carbon nanotube, which is fabricated by peeling off its outer layers, is one of the most interesting nanostructures (Figure 9). In this work, we fabricate the telescoping structure by peeling off its outer layers of a MWNT though destructive fabrication process.

Single MWNT is picked up on the tungsten probe, which is etched by forces-ion-beam (FIB) inside a SEM by the electron-beam-induced deposition (EBID) technique. The MWNTs are synthesized by arc discharge method [43]. One end of a CNT is fixed on an AFM cantilever by EBID [44], [45]. One end of MWNT is freed, and the other end is fixed by EBID. This probe is fixed on the passively driven TEM sample stage. Another tungsten probe etched by the FIB is fixed on the TEM manipulator as an anode. The MWNT is set to the position using the TEM sample stage driven by a SEM manipulator within the working area of the TEM manipulator. Then the free end is also fixed on the tungsten probe fixed TEM manipulator by EBID inside a TEM by controlling its spot size as ~100 nm. After both side fixations, the tungsten probe fixed on the TEM manipulator is moved and tensile stress is applied on MWNT. When the tensile stress reaches fracture stress, the outer layers of MWNT are destructed and the inner core is pulled out. We called this the destructive fabrication process.

Figure 10 shows sequential TEM images sequential destructive fabrication process. Figure 10(a) shows one end freed carbon nanotube which is picked up inside SEM on tungsten probe. The external diameter is ~28 nm and internal diameter is ~2 nm from TEM image. The other free end is fixed by EBID inside a TEM on the tungsten probe, which is set on the TEM manipulator. Then, the probe is moved by the TEM

manipulator in the axial direction of a CNT [Figure 10(b)]. Its outer layers are destroyed by tensile stress and the inner core is pulled out [Figure 10(b)]. As shown in Figure 10(c) and Figure 10(d), the inner core is smoothly pulled out. Figure 10(e) shows the inner core pulled out completely. The external diameter of the fabricated inner core is ~9 nm. From these in-situ experiments, we confirmed that the carbon nanotube is certainly peeled off its outer layers.

NANOACTUATION OF TELESCOPING NANOTUBE BY ELECTROSTATIC FIELDS

The electrostatic actuation of telescoping MWNT is directly observed inside a TEM. In this work, one-end opened MWNT is used for one directional actuation. The schematic diagram of an experimental setup is shown in Figure 11. The other end is fixed on the substrate by the EBID technique. The telescoping structure is set against another probe as an anode inside a TEM by the nanomanipulator. Electrostatic force F_E is generated at the tip of an inner core by applied bias voltage. The circuit current is measured to detect the field emission current form telescoping structure. On increasing the applied voltage, the inner core is actuated by the electrostatic force F_E in its axial direction. The sliding resistance force F_R and van der Waals force F_W are worked on the inner core. The sliding resistance force F_R is quite low, and it is lower than van der Waals forces F_W from the experimental results. Hence, when the electrostatic force F_E is removed, the inner core can be automatically retracted inside outer layers by van der Waals forces F_W.

The telescoping structure is destructively fabricated inside a TEM. The outer layers are fabricated as ~6.6 nm from ~8.4 nm. After positioning against the anode on a TEM manipulator, dc bias voltage is applied. The distance between tungsten probes G_E is fixed as ~1.2 μm. Figure 12 shows the sequence TEM images at each applied voltage. It is clearly observed that the length of inner core l_i is extended and retracted depending on the applied voltage. The length of outer layers l_o is also

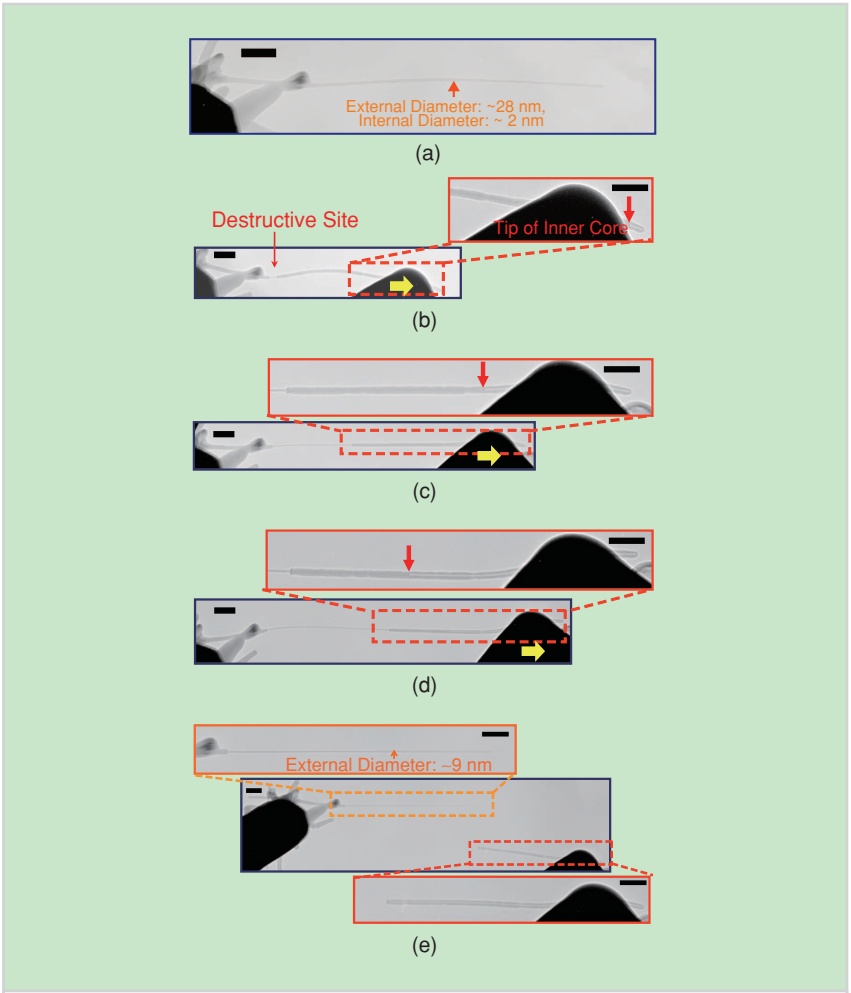

FIGURE 10 Sequential TEM photographs of destructive fabrication of a multi-walled carbon nanotube (Scale bar: 100 nm). (a) Before free end fixation, (b) at the moment of destructive fabrication, (c) during pulling out its inner core, (d) during pulling out its inner core, and (e) after destructive fabrication.

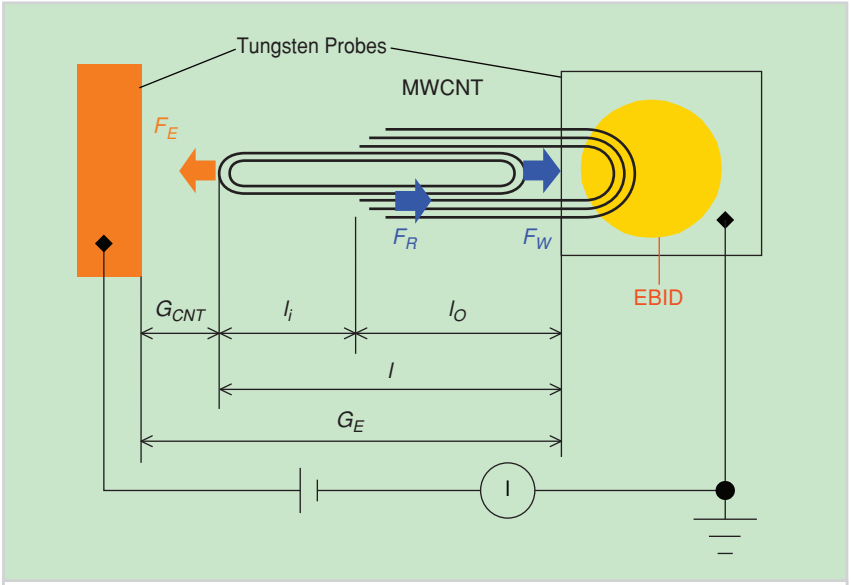

FIGURE 11 Schematic diagram of electrostatic actuation of telescoping MWNT.

increased and decreased by applied voltage. On increasing the applied voltage, the telescoping MWNT is deflected on the concentrated electric field.

SOME 3-D ASSEMBLY REQUIRED

As a typical nanomaterial, the CNTs have been widely investigated to show their extraordinarily mechanical, electronic and chemical properties. Recently, nanotubes have been proposed as a basic building block for the next generation of nanoelectronic and mechanical systems [46], [47]. Their lengths are one of the important parameters for the fabrication and assembly of nanodevices based on CNTs. A number of cutting techniques of CNTs have been proposed previously [48]–[53]. We present a technique for high-speed cutting of CNTs inside an FE-SEM by introducing oxygen gas into the vicinity of the samples [54]. The presence of oxygen gas can be readily used for the bending of CNTs by controlling the irradiation of the electron beam. Here, 3-D nanostructure is assembled using a CNT with a bending technique [55].

CUTTING OF CARBON NANOTUBE BY OXYGEN GAS

Figure 13 shows the cutting procedure of a single CNT at high speed in the presence of oxygen and with the gas nozzle at 90 μm from the samples. The multiwalled CNTs with 20∼50 nm diameters were synthesized by the standard arc-discharge method [43]. We fixed a bundle of CNTs on a stage using electrically conductive tape. Oxygen gas (purity of 99.99995%) was introduced into the vicinity of the sample through a glass nozzle with a 20-μm opening at the end and was regulated by a digital mass flow controller. The CNTs were observed using an acceleration voltage of 5 kV and cut normally using 1 kV inside the FESEM. We selected the spot mode of the electron beam to cut the CNTs. The vacuum in the specimen chamber was reduced from 10^{-4} to 10^{-2} Pa when oxygen gas was introduced at 1 sccm. In order to observe clearly where the cutting occurs on a CNT, TEM images were taken before and after the cutting process in a JEOL 2100 TEM using an acceleration voltage of 200 kV.

A single CNT was cut by the electron beam in the presence of oxygen gas. Cutting was performed using the same electron beam current and acceleration voltage as the two previous cases. The vacuum pressure was 1.6×10^{-2} Pa and the oxygen gas flow rate conditions were the same as previously, however, the nozzle was located at a distance of 90 μm from the CNT in this case. In Figure 14, (a) shows the CNT before cutting, (b) shows the CNT after a length of 650 nm has been cut off, and (c) shows the CNT after removing a further 700 nm. Figure 14(d) details the cutting of a CNT such that it has the same length as the one on the left. These experimental results demonstrate that the length of a CNT can be precisely controlled by cutting using an electron beam, assisted with oxygen gas. The acceleration voltages and the beam currents can cut CNTs in less than one minute. Cutting is easy and rapid at low-acceleration voltages and high beam currents.

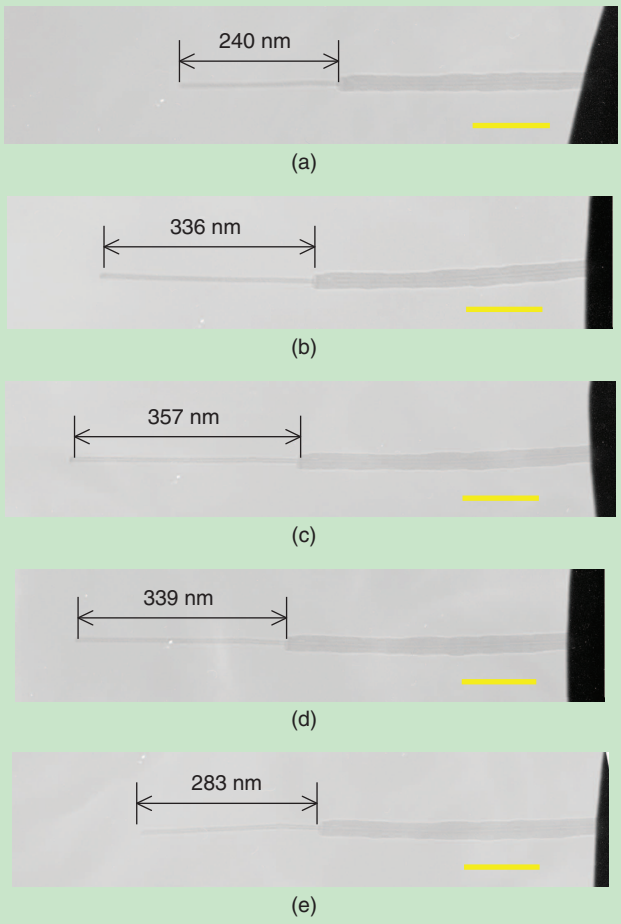

FIGURE 12 Actuation of telescoping MWNT at each applied voltage. (Scale bar: 100 nm) (a) 24.2 V, (b) 44.1 V, (c) 64.9 V, (d) 27.8 V, and (e) 0V.

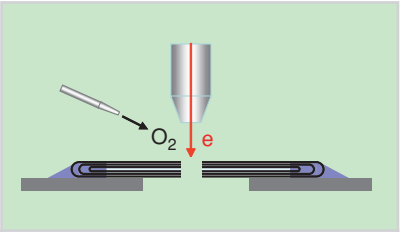

FIGURE 13 The procedure of cutting a single CNT inside a SEM by using an electron beam assisted with oxygen gas.

3D ASSEMBLY OF CARBON NANOTUBE

The presence of oxygen gas in the vicinity of the CNT can also be used for the bending of a CNT. The only changes needed in the process conditions are the increase of the acceleration voltage or the receding of the oxygen gas nozzle from sample, or reducing the irradiation time. Figure 15 shows the schematic of the experimental setup for bending a CNT. Based on this, the bending of CNTs is assumed to have three typical configurations: rippling, buckling, and pentagon-heptagon mode. The mechanism of bending in the experiment is more likely a pentagon-heptagon induced deformation since no mechanical stress is involved, but the carbon-carbon bonds of hexagonal carbon lattice are destructed and part of carbon molecules are removed by the oxygen molecules.

A 3-D nanostructure is constructed by the electron-beam-induced nanofabrication. The multiwalled CNTs with 20∼50 nm diameters were synthesized by the standard arc-discharge method [43]. Oxygen gas (purity of 99.99995%) was introduced into the vicinity of the sample through a glass nozzle with a 20 μm opening at the end and was regulated by a digital mass flow controller. The CNTs were observed using an acceleration voltage of 5 kV and bent normally using 2 kV inside the FESEM. The gas nozzle was set up a distance of 170 μm from the sample with 1 sccm flow rate.

The assembly progress of the structure is shown step by step in Figure 16. Figure 16(a) includes a CNT picked up by an AFM cantilever and manipulated by the nanorobotic manipulator. The other end of the CNT was fixed on an AFM cantilever surface by a tungsten deposit, produced by the proposed welding technique. The other end was set to touch the surface of another AFM cantilever. The proposed bending technique was applied on the CNT, and, as can be seen in Figure 16(b), the CNT was bent at this point. The direction and angle of bending can be controlled by the manipulator. The first bending was followed by another bend in the other CNT point, as shown in Figure 16(c). The location and orientation of the CNT was changed by the manipulator and the second knick was set to touch the substrate as shown in Figure 16(d). Finally, the CNT was cut at third point, shown in Figure 16(e), and the created 3-D nanostructure was separated from the substrate one. As a result, a letter "*N*" was assembled in a CNT and stands on the substrate at two points, as shown in Figure 16(f). The two points attach the structure on the substrate only by van der Waals force.

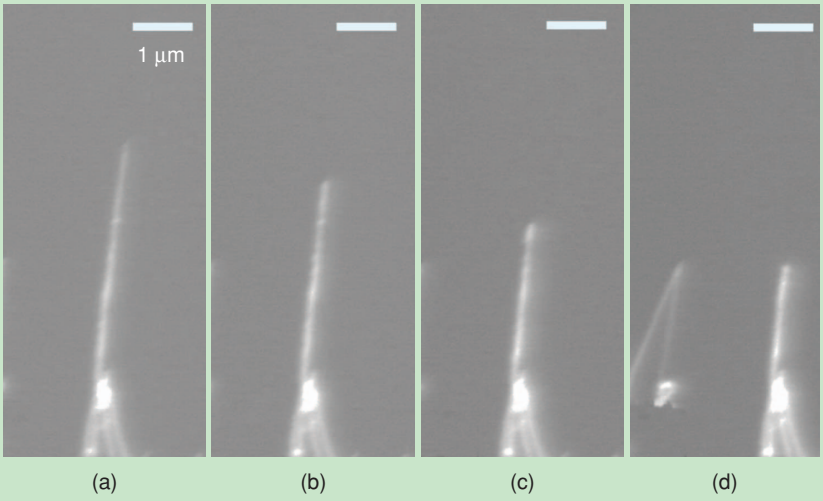

FIGURE 14 (a) Before and (b-d) after cutting of a single CNT in less than one minute. (b) A length of 650 nm was cut off the first time and (c) a further 700 nm was cut off the second time. (d) After cutting, the CNT on the right has the same length as the one on the left.

SINGLE CELL ANALYSIS BASED ON AN E-SEM NANOROBOTIC MANIPULATION SYSTEM

Recently, single-cells analysis has received much more attention because of the progress of the micro/nano scale techniques on the local environmental measurements and controls [56]. Under conventional SEMs and TEMs, the sample chambers of these electron microscopes are set under the high vacuum (HV) to reduce the disturbance of the electron beam for observation. To observe water-containing samples, for example biocells, the appropriate drying and dying treatments are needed before observation. Hence, direct observations of water-containing samples are normally quite difficult through these electron microscopes.

On the other hand, the environmental-SEM (E-SEM) can realize the direct observation of water-containing samples with nanometer high resolution by specially built secondly electron detector [57]. The evaporation of water is controlled by the sample temperature (∼0− ∼40 °C) and sample chamber pressure (10−2,600 Pa). The unique characteristic of the E-SEM is the direct observation of the hydroscopic samples with nondrying treatment. Hence, the nanomanipulation inside the E-SEM is considered to be an effective tool for a water-containing sample with nanometer resolution.

We have been constructed the nanorobotic manipulators inside an E-SEM [58], [59]. The overview of the

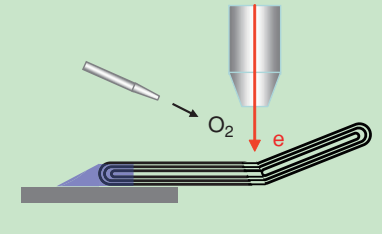

FIGURE 15 Schematic of the experimental setup using an electron beam for bending a nanotube assisted with oxygen gas.

constructed E-SEM nanomanipulator is shown in Figure 17. It has been constructed with three units and seven degrees of freedom in total. The temperature of the sample is controlled by the cooling stage unit, as Unit3. We present that the local stiffness measurement was conducted by using the integrated E-SEM nanomanipulation system for single cell analysis [58].

The cells were fixed on the cooling stage in a perpendicular direction with an AFM cantilever. The AFM cantilever is controlled by the nanomanipulator and is used to apply the compression force on each cell. The E-SEM can provide a real-time observation, i.e., a cell being approached, touched, indented, and finally penetrated/bursted by the AFM cantilever can be seen clearly. As far as this article is concerned, the penetration of a single cell by the AFM cantilever was based on the occurrence of the cell bursting via a real-time observation.

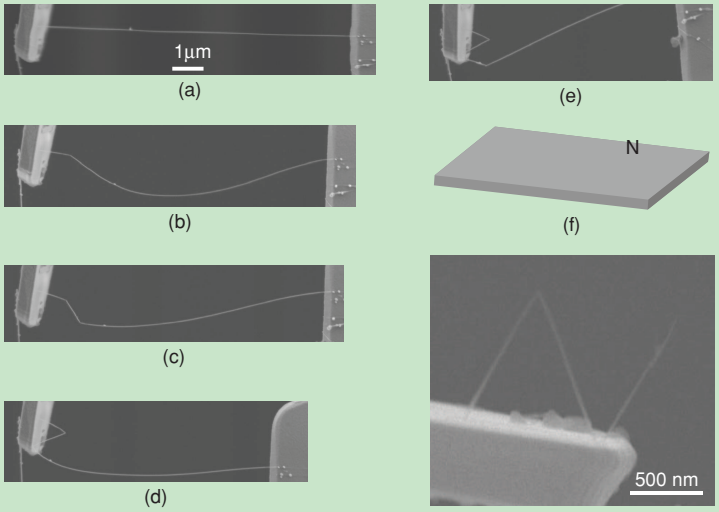

FIGURE 16 Assembly of a 3-D nanostructure based on a CNT assisted with (a) welding, (b)-(d) bending, and (e) cutting techniques. (f) The letter N stands on the substrate.

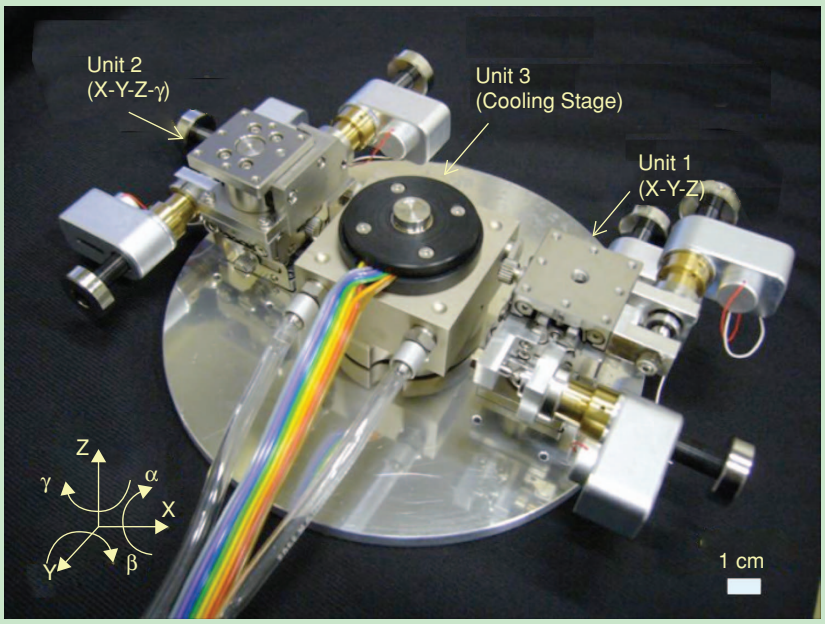

FIGURE 17 Overview of the nanorobotic manipulator of E-SEM.

Force (F)-cantilever indentation (I) curves were determined from the experiment. The value of F was calculated by using (1), where k, φ, and L are the spring constant, the displacement angle in radians, and the length of the cantilever, respectively. Values of φ, L, and I were determined from direct measurements of E-SEM images using an image analysis software (ImageJ, developed at the National Institute of Health), while k was obtained from the manufacturer (Olympus Corp., 0.02 N/m spring constant). Equation (1) was derived from the Hooke's law, i.e., $F = k\delta$, where δ is the displacement of the cantilever which was obtained by using $\delta = \varphi(2/3)L$

$$F = k\varphi(2/3)L. \qquad (1)$$

The Hertz-Sneddon models, which are based on the shape of the tips, i.e., conical, spherical, and cylindrical, were used to estimate the Young's modulus of the cells as expressed in (2), (3). Parameters of E, ν, α, R, and a are the Young's modulus, the Poisson's ratio ($\nu = 0.5$ for soft biological materials [58]) of the elastic half space (cell's surface), the half opening angle of a conical tip, the radius of curvature of a spherical tip, and the radius of a cylindrical tip, respectively. Values for α, R, and a were obtained from E-SEM images. Values for these parameters are summarized in Table 1

$$F_{\text{spherical}} = \frac{4}{3}\frac{E}{(1-\nu^2)}R^{1/2}I^{3/2}. \qquad (2)$$

The models predict that the load depends on the indentation according to a power law related to the tip geometry [58]. In order to choose the correct tip geometry, an equation of the form $F = mI^b$ was fitted to force versus indentation curves using commercial fitting software (DataFit), where the exponent b depends on the tip shape. The final equation of the Young's modulus based on the Hertz-Sneddon models,

i.e., (2), and the parameter's values (Table 1) for three different tip shapes, i.e., conical (HV mode), spherical (E-SEM mode), and cylindrical (E-SEM mode and HV mode), are expressed in (3)

$$E_{\text{cell}} = (3.977 \times 10^3)\frac{F_{\text{spherical}}}{I^{3/2}}. \quad (3)$$

The E-SEM photo during penetrations of single yeast cells is shown in Figure 19. The penetration forces clearly show a strong relationship between cell size and strength, the latter increases with an increase in cell size as shown in Figure 20. The average penetration forces for 3, 4, 5, and 6 μm cell diameter ranges are 96 ± 2, 124 ± 10, 163 ± 1, and 234 ± 14 nN, respectively. Yeast cell walls consist predominantly of glucan with (1,3)-β and (1,6)-β linkages, and mannan covalently linked to protein (mannoprotein) [60]–[62]. Thus it can be inferred that the β-glucans composition increases when the yeast cell size increases. The average Young's modulus obtained in this work, i.e., 3.24 ± 0.09 MPa, is reasonable compared to reported local cell stiffness values of 0.73 MPa [63] and 1.12 MPa [59], since the E values obtained in this paper represent not only the local elastic property of the cell but also the whole cell stiffness.

CONCLUSIONS AND FUTURE DIRECTIONS

A nanolaboratory based on a nanorobotic manipulation system has been presented where the hybrid nanorobotic manipulation system is integrated with a nanorobotic manipulator inside a TEM and an SEM. The electrostatic actuation of telescoping MWNT was directly observed inside a TEM. The telescoping MWNT was fabricated by peeling off outer layers through the destructive fabrication process. A cutting technique for CNTs assisted by the presence of oxygen gas has been also presented. The cutting procedure was conducted in less than one minute using a low-energy electron beam inside a scanning electron microscope. A bending technique of a CNT assisted by the presence of oxygen gas was applied for the 3-D fabrication of the nanosturucture. The stiffness measurements for single cell analysis have been also presented based on an E-SEM nanorobotic manipulation system.

A nanolaboratory is considered to be a powerful tool for future applications of nanoassembly and nanoinstrumentation (Figure 21). For the next steps of nanomanipulations, mainly two directions can be expected. The first direction is the improvement and development of the manipulation system for automatic assembly of nanoscale objects. The

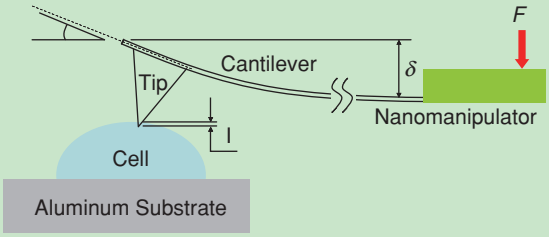

FIGURE 18 Schematics of sinlge cell stiffness measurements through nanorobotic manipulation system.

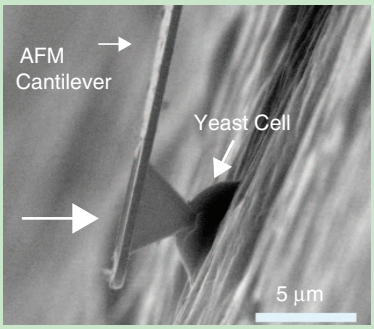

FIGURE 19 E-SEM photo during the penetration experiments of single yeast cells by an AFM cantilever tip.

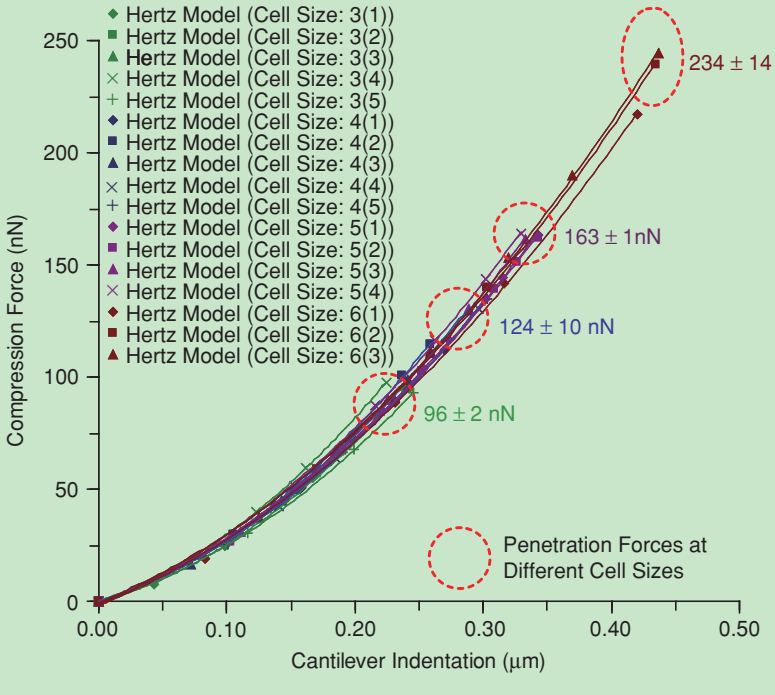

FIGURE 20 Penetration force using a sharp tip at different cell sizes. Experimental data are fitted using the spherical model. The curves are shown until the penetration points. Inner bracket () indicates the cell number for each cell size. Cell size is in μm.

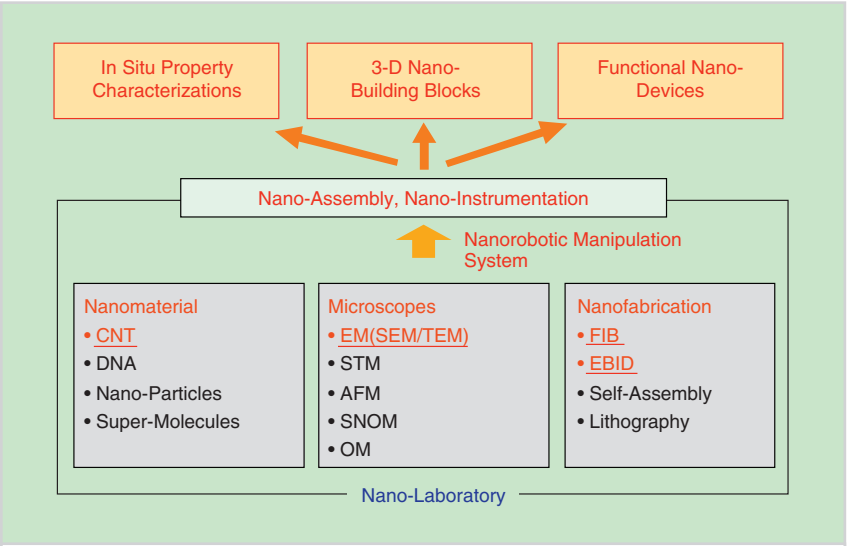

FIGURE 21 Nanolaboratory based on a nanorobotic manipulation system for future applications of nanoassembly and nanoinstrumentation.

building-up techniques from atomic scale are also desirable to assemble novel effective nanostructures and nanodevices. The bottom-up techniques, such as self assembly techniques, have the potential to apply the nanomanipulation for the bottom-up nanoassembly [64]. The second direction is to realize and construct various useful nanodevices by nanomanipulation techniques using different types of nanomaterials. CNTs have been considered one priority for the future nanodevices. For examples, nanotweezers [46], shaped STM tip [65], [66], mechanical memory [67], rotational actuator [68], single electron transistor [69], field-effect transistors (FETs) [70], field emitter [71], [72], field emission microscopy (FEM) [73], gas chemical sensors [74], hydrogen storages [75], nanothemometers [76], flow sensors [77], SEM cathodes of field-emission emitter to develop the miniaturized SEM system [78], [79], x-ray source based on their field emitters [80], have been proposed for these attractive nanodevices. Nanobio application has included such desired applications using nanodevices.

ACKNOWLEDGMENTS

The authors are grateful to Prof. Y. Saito at Nagoya University for providing us with MWNTs and Prof. T. Inada N. Uozumi for providing *W303* yeast cells. This work was partially supported by a grant-in-aid for scientific research from the Ministry of Education, Culture, Sports, Science, and Technology of Japan.

REFERENCES

[1] R.P. Feynman, "There's plenty of room at the bottom," *Caltech's Engin. Sci.*, vol. 23, pp. 22–36, 1960.

[2] K.E. Drexler, *Engines of Creation*. New York: Anchor Books, 1986.

[3] K.E. Drexler, *Nanosystems: Molecular Machinery, Manufacturing, and Computation*. New York: Wiley Interscience, 1992.

[4] T. Fukuda, F. Arai, and L.X. Dong, "Assembly of nanodevices with carbon nanotubes through nanorobotic manipulations," *Proc. IEEE*, vol. 91, no. 11, 2003, pp. 1803–1818.

[5] R.W. Siegel, E. Hu, and M.C. Roco, *Nanostructure Science and Technology*. Norwell, MA: Kluwer Academic Publishers, 1999.

[6] H.G. Craighead, "Nanoelectromechanical systems," *Science*, vol. 290, no. 5496, pp. 1532–1535, 2000.

[7] M. Staples, K. Daniel, M.J. Sima, and R. Langer, "Applications of micro- and nano-electromechanical devices to drug delivery," *Pharnaceutical Res.*, vol. 23, no. 5, pp. 847–863, 2006.

[8] S.P. Leary, C.Y. Liu, and M.L.J. Apuzzo, "Toward the emergence of nanoneurosurgery: Part III—nanomedicine: Targeted nanotherapy, nanosurgery, and progress toward the realization of nanoneurosurgery," *Neurosurgery*, vol. 58, no. 6, pp. 1009–1026, 2006.

[9] E. Du, H. Cui, and Z. Zhu, "Review of nanomanipulators for nanomanufacturing," *Int. J. Nanomanufacturing*, vol. 1, no. 1, pp. 83–104, 2006.

[10] S.W. Hell, "Far-field optical nanoscopy," *Science*, vol. 316, no. 5828, pp. 1153–1158, 2007.

[11] D.M. Eigler and E.K. Schweizer, "Positioning single atoms with a scanning electron microscope," *Nature*, vol. 344, pp. 524–526, Apr. 1990.

[12] S. Hosoki, S. Hosaka, and T. Hasegawa, "Surface modification of MoS2 using STM," *Appl. Surf. Sci.*, vol. 60/61, pp. 643–647, 1992.

[13] T. Hertel, R. Martel, and P. Avouris, "Manipulation of individual carbon nanotubes and their interaction with surfaces," *J. Phys. Chem. B*, vol. 102, no. 6, pp. 910–915, 1998.

[14] G. Li, N. Xi, H. Chen, C. Poneroy, and M. Prokos, "Videolized atomic force microscopy for interactive nanomanipulation and nanoassembly," *IEEE Trans. Nanotech.*, vol. 4, no. 5, pp. 605–615, 2005.

[15] G. Li, N. Xi, M. Yu, and W.-K. Fung, "Development of augmented reality system for afm based nanomanipualiton," *IEEE Trans. Mechatronics.*, vol. 9, no. 2, pp. 358–365, 2004.

[16] M. Sitti and H. Hashimoto, "Teleoperated touch feedback from the surfaces at the nanoscale: Modeling and experiments," *IEEE Trans. Mechatronics*, vol. 8, no. 2, pp. 287–298, 2003.

[17] T. Ando, N. Kodera, Y. Naito, T. Kinoshita, K. Fukuda, Y. Toyoshima, "A high-speed atomic force microscope for studying biological macromolecules in action," *Proc. Nat. Acad. Sci.*, vol. 98, no. 22, 2003, pp. 12468–12472.

[18] T. Ando, T. Uchihashi, N. Kodera, D. Yamamoto, A. Miyagi, M. Taniguchi, and H. Yamashita, "High-speed AFM and nano-visualization of biomolecular processes," *Pflugers Archiv European J. Physio.*, vol. 456, no. 1, pp. 211–225, 2008.

[19] M. Nakao, K. Tsuchiya, K. Matsumoto, and Y. Hatamura, "Micro handling with rotational needle-type tools under realtime observation," *Annals CIRP*, vol. 50, no. 1, pp. 9–12, 2001.

[20] S. Saito, H.T. Miyazaki, T. Sato, and K. Takahashi, "Kinematics of mechanical and adhesional micromanipulation under a scanning electron microscope," *J. Appl. Phys.*, vol. 92, no. 6, pp. 5140–5149, 2002.

[21] T. Kasaya, H.T. Miyazaki, S. Saito, K. Koyano, T. Yamaura, and T. Sato, "Image-based autonomous micromanipulation system for arrangement of spheres in a scanning electron microscope," *Rev. Sci. Instrum.*, vol. 75, no. 6, pp. 2033–2042, 2004.

[22] M.F. Yu, O. Lourie, M.J. Dyer, K. Moloni, T.F. Kelley, and R.S. Ruoff, "Strength and breaking mechanism of multiwalled carbon nanotubes under tensile load," *Science*, vol. 287, no. 5453, pp. 637–640, 2000.

[23] T. Kizuka, K. Yamada, S. Deguchi, M. Naruse, and N. Tanaka, "Cross-sectional time resolved high-resolution transmission electron microscopy of atomic-scale contact and noncontact-type scannings on gold surfaces," *Phys. Rev. B*, vol. 55, no. 12, pp. 7398–7401, 1997.

[24] T. Kizuka, S. Umehara, and S. Fujisawa, "Metal-Insulator transition in stable one-dimensional arrangements of single gold atoms," *Jpn. J. Appl. Phys*, vol. 40, no. 1, pp. L71–L74, 2001.

[25] Z.L. Wang, "Properties of nanobelets nad nanotubes measured by In situ TEM," *Microscopy Microanalysis*, vol. 10, no. 1, pp. 158–166, 2004.

[26] M. Nakajima, F. Arai, and T. Fukuda, "In situ fabrication and electric actuation of telescoping nanotube inside tem through hybrid nanorobotic manipulation system," *Proc. 2006 IEEE/RSJ Int. Conf. on Intelligent Robotics Syst. (IROS 2006)*, 2006, pp. 1915–1920.

[27] M. Nakajima, F. Arai, and T. Fukuda, "In situ measurement of Young's modulus of carbon nanotube inside tem through hybrid nanorobotic manipulation system," *IEEE Trans. Nanotechmology*, vol. 5, no. 3, pp. 243–248, 2006.

[28] L.X. Dong, F. Arai, and T. Fukuda, "3D nanorobotic manipulations of multi-walled carbon nanotubes," *Proc. 2001 IEEE Int. Conf. Robot. Automat. (ICRA2001)*, 2001, pp. 632–637.

[29] L.X. Dong, F. Arai, and T. Fukuda, "Destructive constructions of nanostructures with carbon nanotubes through nanorobotic manipulation," *IEEE Trans. Mechatron.*, vol. 9, no. 2, pp. 350–357, 2004.

[30] S. Iijima, "Helical microtubules of graphitic carbon," *Nature*, vol. 354, pp. 56–58, Nov. 1991.

[31] P.G. Collins and P. Avouris, "Nanotubes for electronics," *Sci. Amer.*, vol. 283, pp. 62–69, Dec. 2000.

[32] D. Qian, G.J. Wagner, and W.K. Liu, "Mechanics of carbon nanotubes," *Appl. Mech. Rev.*, vol. 55, no. 6, pp. 495–533, 2002.

[33] J.P. Lu, "Elastic properties of carbon nanotubes and nanoropes," *Phys. Rev. Lett.*, vol. 79, no. 7, pp. 1297–1300, 1997.

[34] E.W. Wong, P.E. Sheehan, and C.M. Lieber, "Nanobeam mechanics: Elasticity, strength, and toughness of nanorods and nanotubes," *Science*, vol. 277, No. 5334, pp. 1971–1975, 1997.

[35] Y. Saito, T. Yoshikawa, S. Bandow, M. Tomita, and T. Hayashi, "Interlayer spacings in carbon nanotubes," *Phys. Rev. B*, vol. 48, no. 3, pp. 1907–1909, 1993.

[36] O. Zhou, R.M. Fleming, D.W. Murphy, C.H. Chen, R.C. Haddon, A.P. Ramirez, and S.H. Glarum, "Defects in carbon nanotubes," *Science*, vol. 263, no. 5154, pp. 1744–1747, 1994.

[37] J. Cumings and A. Zettl, "Low-friction nanoscale linear bearing realized from multiwall carbon nanotubes," *Science*, vol. 289, no. 5479, pp. 602–604, 2000.

[38] A.M. Fennimore, T.D. Yuzvinssky, W.Q. Han, M.S. Fuhrer, J. Cummings, and A. Zettl, "Rotational actuators based on carbon nanotubes," *Nature*, vol. 424, pp. 408–410, June 2003.

[39] Q. Zheng and Q. Jiang, "Multiwalled carbon nanotubes as gigahertz oscillators," *Phys. Rev. Lett.*, vol. 88, no. 4, p. 045503, 2002.

[40] A. Hansson and S. Stafstrom, "Intershell conductance in multiwall carbon nanotubes," *Phys. Rev. B.*, vol. 67, no. 7, p. 075406, 2003.

[41] M. Nakajima, S. Arai, Y. Saito, F. Arai, and T. Fukuda, "Nanoactuation of telescoping multi-walled carbon nanotubes inside transmission electron microscope," *Jpn. J. Appl. Phys.*, vol. 46, no. 42, pp. L1035–L1038, 2007.

[42] L.X. Dong, B.J. Nelson, F. Arai, T. Fukuda, "Towards nanotube linear servomotors," *IEEE Trans. Automation Sci. Eng.*, vol. 3, no. 3, pp. 228–235, 2006.

[43] Y. Saito, T. Yoshikawa, and M. Inagaki, "Growth and structure of graphitic tubules and polyhedral particles in arc-discharge," *Chem. Phys. Lett.*, vol. 204, no. 3.4, pp. 277–282, 1993.

[44] H.W.P. Koops, J. Kretz, M. Rudolph, M. Weber, G. Dahm, and K.L. Lee, "Characterization and application of materials grown by electron-beam-induced deposition," *Jpn. J. Appl. Phys.*, vol. 33, no. 12B, pp. 7099–7107, 1994.

[45] L.X. Dong, F. Arai, and T. Fukuda, "Electron-beam-induced deposition with carbon nanotube emitters," *Appl. Phys. Lett.*, vol. 81, no. 10, pp. 1919–1921, 2002.

[46] P. Kim and C.M. Lieber, "Nanotube nanotweezers," *Science*, vol. 286, pp. 2148–2150, Dec. 1999.

[47] P.G. Collins, M.S. Arnold, and P. Avouris, "Engineering carbon nanotubes and nanotube circuits using electrical breakdown," *Science*, vol. 292, no. 5447, pp. 706–709, 2001.

[48] H. Dai, J.H. Hafner, A.G. Rinzler, D.T. Colbert, and R.E. Smalley, "Nanotubes as nanoprobes in scanning probe microscopy," *Nature*, vol. 384, pp. 147–150, Nov. 1996.

[49] T. Belytschko, S.P. Xiao, G.C. Schatz, and R.S. Ruoff, "Atomistic simulations of nanotube fracture," *Rhys. Rev. B*, vol. 65, no. 23, p. 235430, 2002.

[50] M. Sammalkorpi, A. Krasheninnikov, A. Kuronen, K. Nordlund, and K. Kaski, "Mechanical properties of carbon nanotubes with vacancies and related defects," *Phys. Rev. B*, vol. 70, no. 70, p. 245416, 2004.

[51] A. Subramaniam, L.X. Dong, D. Frutiger, and B.J. Nelson, "Shell engineering of carbon nanotube array by current driven breakdown," *Proc. IEEE Conf. Nanotechnolgy (IEEE-Nano 2006)*, 2006, pp. 901–904.

[52] S. Suzuki, K. Kanzaki, Y. Homma, and S. Fukuba, "Low-acceleration-voltage electron irradiation damage in single-walled carbon nanotubes," *Jpn. J. Appl. Phys.*, vol. 43, no. 8B, pp. L1118–L1120, 2004.

[53] T.D. Yuzvinsky, A.M. Fennimore, W. Mickelson, C. Esquivias, and A. Zettl, "Precision cutting of nanotubes with a low-energy electron beam," *Appl. Phys. Lett.*, vol. 86, p. 053109, Jan. 2005.

[54] P. Liu, F. Arai, and T. Fukuda, "Cutting of carbon nanotubes assisted with oxygen gas inside a scanning electron microscope," *Appl. Phys. Lett.*, vol. 89, p. 113104, Sept. 2006.

[55] P. Liu, K. Kantola, T. Fukuda, and F. Arai, "Cutting of carbon nanotubes assisted with oxygen gas inside a scanning electron microscope," *Proc. IEEE Int. Conf. Robot. Automat. (ICRA2007)*, 2007, pp. 441–446.

[56] S.P. Leary, C.Y. Liu, and M.L.J. Apuzzo, "Toward the emergence of nanoneurosurgery," *Neurosurgery*, vol. 58, pp. 1009–1026, 2006.

[57] M. Nakajima, F. Arai, and T. Fukuda, "Nanofixation with Low Melting Metal Based on Nanorobotic Manipulation," *Proc. 2006 Sixth IEEE Conf. Nanotechnology (IEEE-Nano 2006)*, 2006, pp. 925–928.

[58] M.R. Ahmad, M. Nakajima, S. Kojima, M. Homma, and T. Fukuda, "In-situ single cell mechanical characterization of W303 yeast cells inside environmental-SEM," *Proc. 7th IEEE Int. Conf. Nanotechnology (IEEE-Nano 2007)*, 2007, pp. 1022–1027.

[59] T.S. Laneroa, O. Cavalleria, S. Krol, R. Rolandi, and A. Gliozzi, "Mechanical properties of single living cells encapsulated in polyelectrolyte matrixes," *J. Biotech.*, vol. 124, no. 4, pp. 723–731, 2006.

[60] F.M. Klis, A. Boorsma, and P.W.J. De Groot, "Cell wall construction in *saccharomyces cerevisiae*," *Yeast*, vol. 23, no. 3, pp. 185–202, 2006.

[61] G. Lesage and H. Bussey, "Cell wall assembly in saccharomyces cerevisiae," *Microbiology and Molecular Biology Rev.*, vol. 70, no. 2, pp. 317–343, 2006.

[62] P.N. Lipke and R. Ovalle, "Cell wall architecture in yeast: new sturcture and new challenges," *J. Bacteriology*, vol. 180, no. 15, pp. 3735–3740, 1998.

[63] A.E. Pelling, S. Sehati, E.B. Gralla, J.S. Valentine, J.K. Gimzewski, "Local nanomechanical motion of the cell wall of saccharomyces cerevisiae," *Science*, vol. 305, no. 5687, pp. 1147–1150, 2004.

[64] G.M. Whitesides and B. Grzybowski, "Self-assembly at all scales," *Science*, vol. 295, no. 5564, pp. 2407–2409, 2002.

[65] H. Dai, J.H. Hafner, A.G. Rinzler, D.T. Colbert, and R.E. Smally, "Nanotubes as nanoprobes in scanning probe microscopy," *Nature*, vol. 384, pp. 147–150, Nov. 1996.

[66] S. Akita, H. Nishijima, Y. Nakayama, F. Tokumasu, and K. Takeyasu, "Carbon nanotube tips for a scanning probe microscope: Their fabrication and properties," *J. Phys D: Appl. Phys.*, vol. 32, no. 9, pp. 1044–1048, 1999.

[67] T. Rueckes, K. Kim, E. Joselevich, G.Y. Tseng, C.-K. Cheung, and C.M. Lieber, "Carbon nanotube-based nonvolatile random access memory for molecular computing," *Science*, vol. 289, no. 5476, pp. 94–197, 2000.

[68] A.M. Fennimore, T.D. Yuzvinsky, W.-Q. Han, M.S. Fuhrer, J. Cumings, and A. Zettl, "Rotational actuators based on carbon nanotubes," *Nature*, vol. 424, pp. 408–410, July 2003.

[69] H.W. Ch. Postma, T. Teepen, Z. Yao, M. Grifoni, and C. Dekker, "Carbon nanotube single-electron transistors at room temperature," *Science*, vol. 293, no. 5527, pp. 76–79, 2001.

[70] A. Bachtold, P. Hadley, T. Nakanishi, and C. Dekker, "Logic circuits with carbon nanotube transistors," *Science*, vol. 294, no. 5545, pp. 1317–1320, 2001.

[71] A.G. Rinzler, J.H. Hafner, P. Nikolaev, L. Lou, S.G. Kim, D. Toma'nek, P. Nordlander, D.T. Colbert, and R.E. Smalley, "Unraveling nanotubes: Field emission from an atomic wire," *Science*, vol. 269, no. 5230, pp. 1550–1553, 1995.

[72] W.A. de Heer, A. Chatelain, and D. Ugarte, "A carbon nanotube field emission electron source," *Science*, vol. 270, no. 5239, pp. 1179–1180, 1995.

[73] Y. Saito, K. Hamaguchi, K. Hata, K. Uchida, Y. Tasaka, F. Ikazaki, M. Yumura, A. Kasuya, and Y. Nishima, "Conical beams from open nanotubes," *Nature*, vol. 389, pp. 554–555, Oct. 1997.

[74] J. Kong, N.R. Franklin, C. Zhou, M.G. Chapline, S. Peng, K. Cho, and H. Dai, "Nanotube molecular wires as chemical sensors," *Science*, vol. 287, no. 5453, pp. 622–625, 2000.

[75] C. Liu, Y.Y. Fan, M. Liu, H.T. Cong, H.M. Cheng, and M.S. Dresselhaus, "Hydrogen storage in single-walled carbon nanotubes1 at room temperature," *Science*, vol. 286, no. 5542, pp. 1127–1129, 1999.

[76] Y. Gao and Y. Bando, "Carbon nanothermometer containing gallium," *Nature*, vol. 415, pp. 599–600, Feb. 2002.

[77] S. Ghosh, A.K. Sood, and N. Kumar, "Carbon nanotube flow sensors," *Science*, vol. 299, no. 5609, pp. 1042–1044, 2003.

[78] H. Suga, H. Abe, M. Tanaka, T. Shimizu, T. Ohno, Y. Nishioka, and H. Tokumoto, "Stable multiwalled carbon nanotube electron emitter operating in low vacuum," *Surf. Interface Anal.*, vol. 38, no. 12–13, pp. 1763–1767, 2006.

[79] R. Yabushita, K. Hata, and H. Sato, and Y. Saito, "Development of compact field emission scanning electron microscope equipped with multiwalled carbon nanotube bundle cathode," *J. Vac. Sci. Technol. B*, vol. 25, no. 2, pp. 640–642, 2007.

[80] J. Zhang, G. Yang, Y. Cheng, B. Gao, Q. Qiu, Y.Z. Lee, J.P. Lu and O. Zhoua, "Scanning x-ray source based on carbon nanotube field emitters," *Appl. Phys. Lett.*, vol. 86, p. 184104, Apr. 2005.

ABOUT THE AUTHORS

Toshio Fukuda (fukuda@mein.nagoya-u.ac.jp) received his M.S. and Dr. Eng. degrees from the University of Tokyo, Japan, in 1973 and 1977, respectively. He works as the professor of the Department of Micro-Nano Systems Engineering at Nagoya University, Nagoya, Japan, and currently serves as the AdCom past president of IEEE Nanotechnology Council.

Masahiro Nakajima (nakajima@mein.nagoya-u.ac.jp) received his M.S. and Dr. Eng. degrees from Nagoya University, Nagoya, Japan, in 2003 and 2006, respectively. He is an assistant professor of the Department of Micro-Nano Systems Engineering.

Pou Liu (liupou@robo.mein.nagoya-u.ac.jp) received his M.S. and Dr. Eng. degrees from Nagoya University, Nagoya, Japan, in 2004 and 2007, respectively. He is currently a postdoctoral researcher in the Department of Micro-Nano Systems Engineering, Nagoya University.

Mohd Ridzuan Ahmad (ridzuan@robo.mein.nagoya-u.ac.jp) received his M.S. Eng. degree from Universiti Teknologi Malaysia (UTM) in 2003 and is currently working toward his Ph.D. degree in nano-bio manipulation systems at Nagoya University. N